Unresolved Plasma Motions in Coronal Loops

Hirohisa Hara

National Astronomical Observatory of Japan

Coronal Loop Workshop VII in University of Cambridge

Introduction

- The non-thermal broadening of coronal emission lines is the central topic of this study.

- It has been pointed out by the Climax coronagraph observation ($T_i^* > T_e$; Billings & Lehman 1962).

- It has been investigated extensively by the spacecraft observations starting in the Skylab era ($T_i \sim T_e$, ξ ; Boland+ 1975, Doschek+ 1976, Cheng+ 1979).

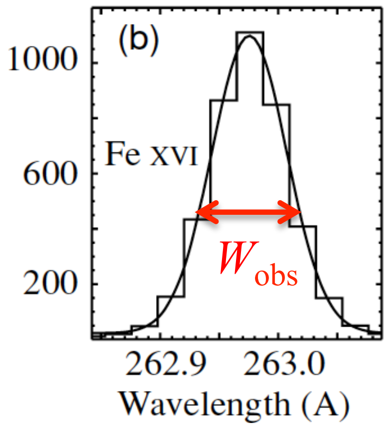

$$W_{obs}^2 = W_I^2 + W^2$$
$$= W_I^2 + 4\ln 2\left(\frac{2kT_i}{M_i} + \xi^2\right)$$

(in velocity unit) $= 2kT_i^*/M_i$

W_{obs}: observed FWHM in a line
W_{instr}: FWHM of instrument origin
T_i : ion temperature
M_i : mass of ion
ξ : non-thermal velocity

$$T_i^*(M_i) \neq T_i^*(M_j)$$

for lines formed at similar T_e

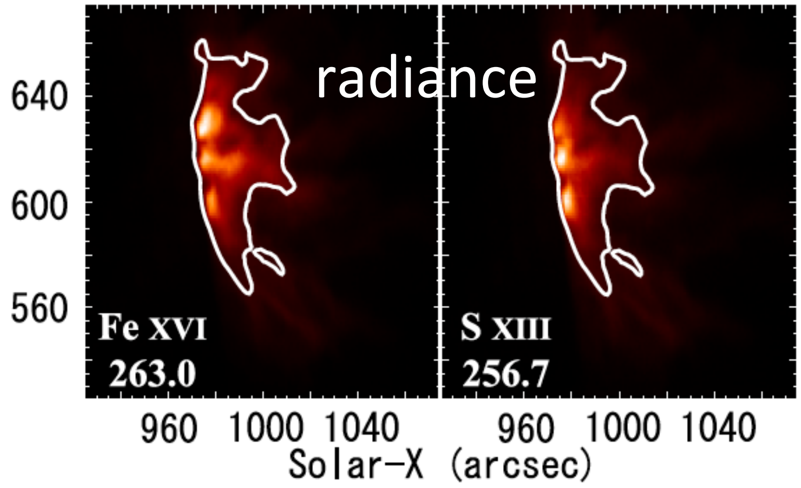

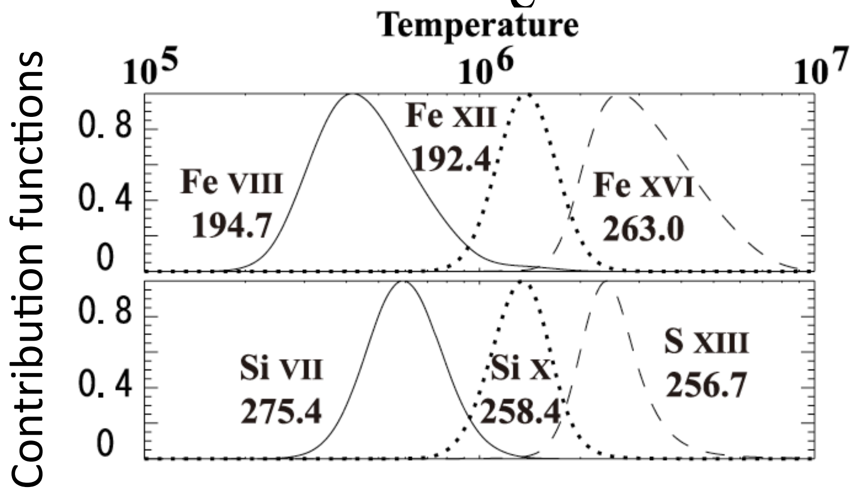

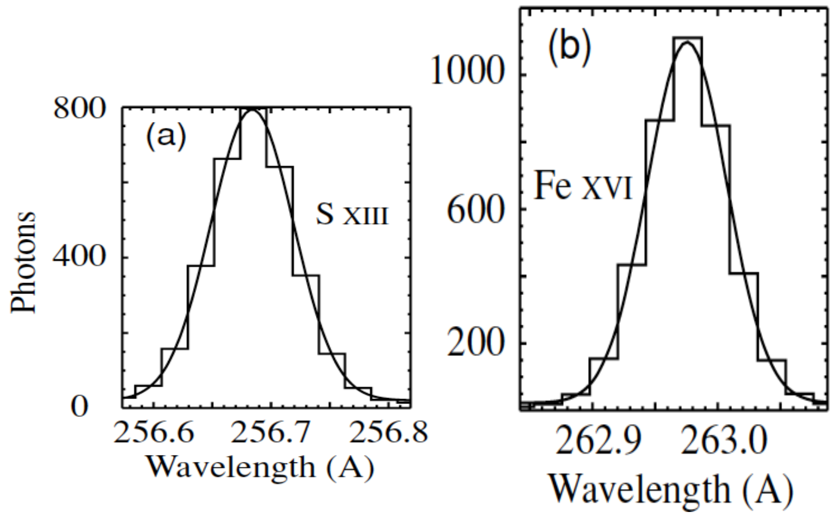

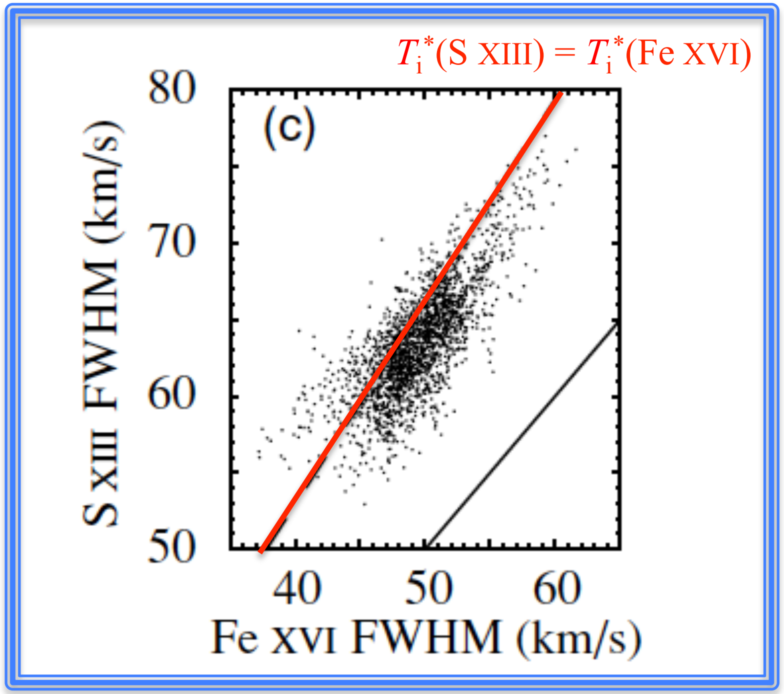

Imada, Hara, Watanabe (2009)

Non-thermal velocity ξ or $V_{\rm NT}$

- $\xi \propto T_e^{1/4}$ in Transition Region

Const. of acoustic energy flux

$$\phi_S = \rho \xi^2 V_s \quad (\text{ergs cm}^{-2}\ \text{s}^{-1})$$
$$= 4.4 \times 10^5 \left(\frac{\xi}{20\ \text{km s}^{-1}}\right)^2 \left(\frac{P}{1\ \text{dyn cm}^{-2}}\right) \times \left(\frac{T_e}{10^6\ \text{K}}\right)^{-1/2}$$

Const. of Alfven energy flux

$$\phi_F = \rho \xi^2 V_A \quad (\text{ergs cm}^{-2}\ \text{s}^{-1})$$
$$= 9.6 \times 10^6 \left(\frac{\xi}{20\ \text{km s}^{-1}}\right)^2 \left(\frac{P}{1\ \text{dyn cm}^{-2}}\right)^{1/2} \times \left(\frac{T_e}{10^6\ \text{K}}\right)^{-1/2} \left(\frac{B}{100\ \text{G}}\right)$$

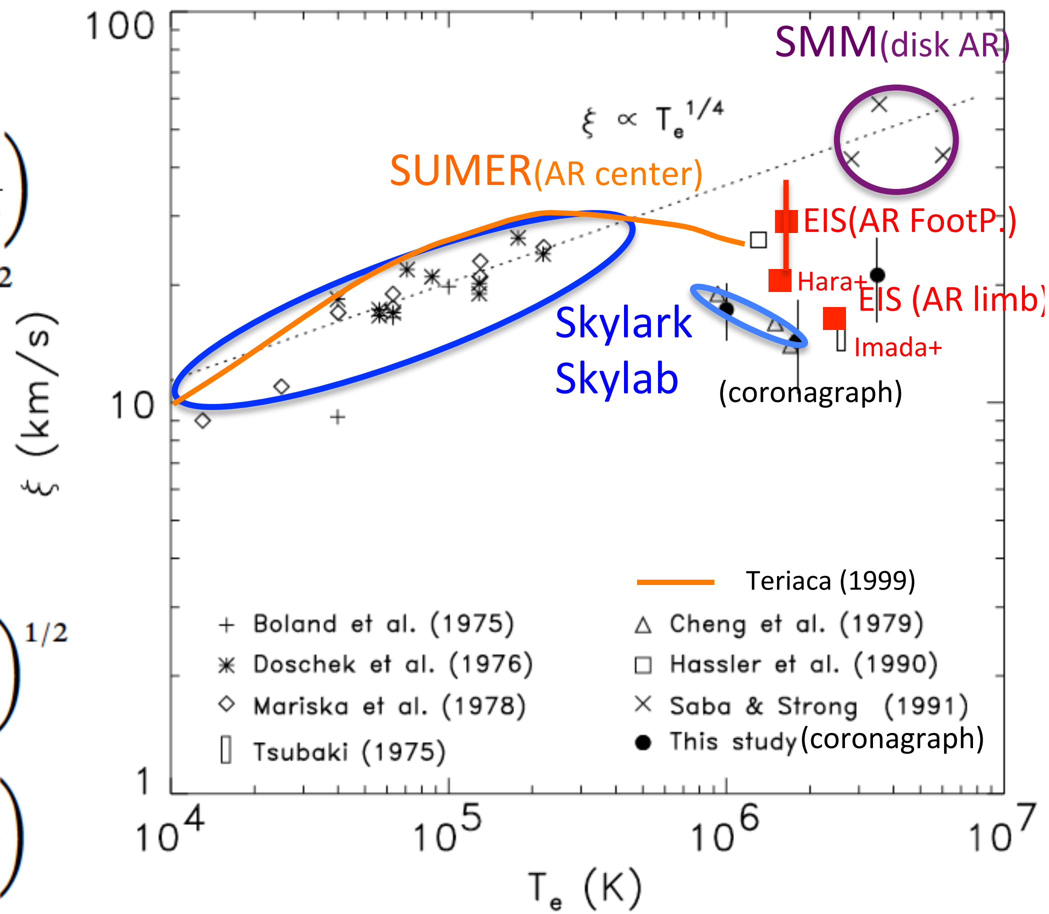

Hara & Ichimoto (1999)

Non-thermal velocity ξ or V_{NT}

- Interpretation
  - Increase of T_{i} by heating ions (will not be the case)

  - Multiple components with different bulk Doppler velocity along the line of sight

  - Unresolved motion
    - Small-scale multiple flows/motions
    - Motion of magnetic structures including waves
    - Turbulence

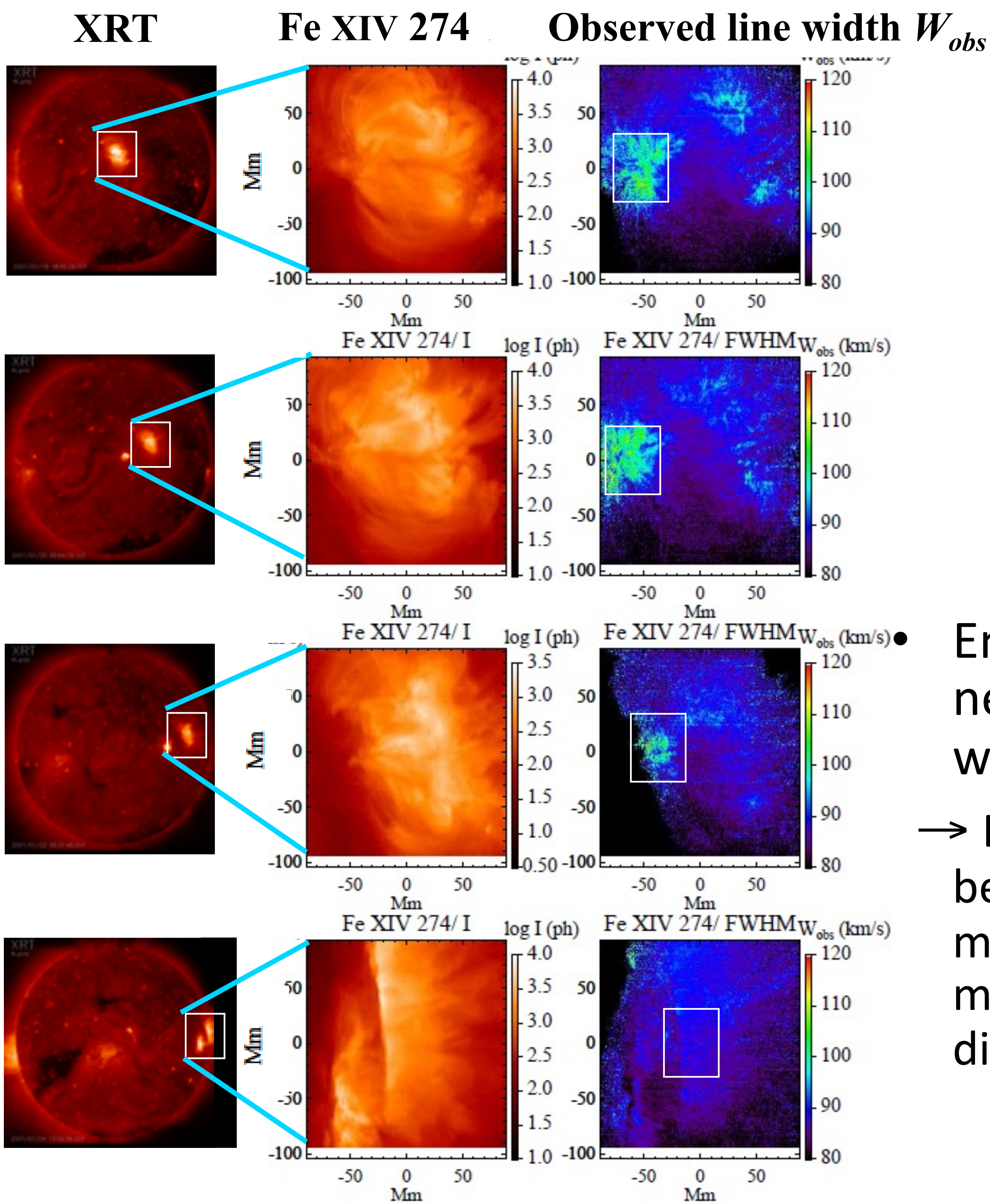

Line width change with rotation

- Enhanced line broadening near footpoints disappears with rotation.

→ Excess line broadening may be due to superposition of multiple components along magnetic field line, each with different line centers.

Unresolved Flows

hidden in line width

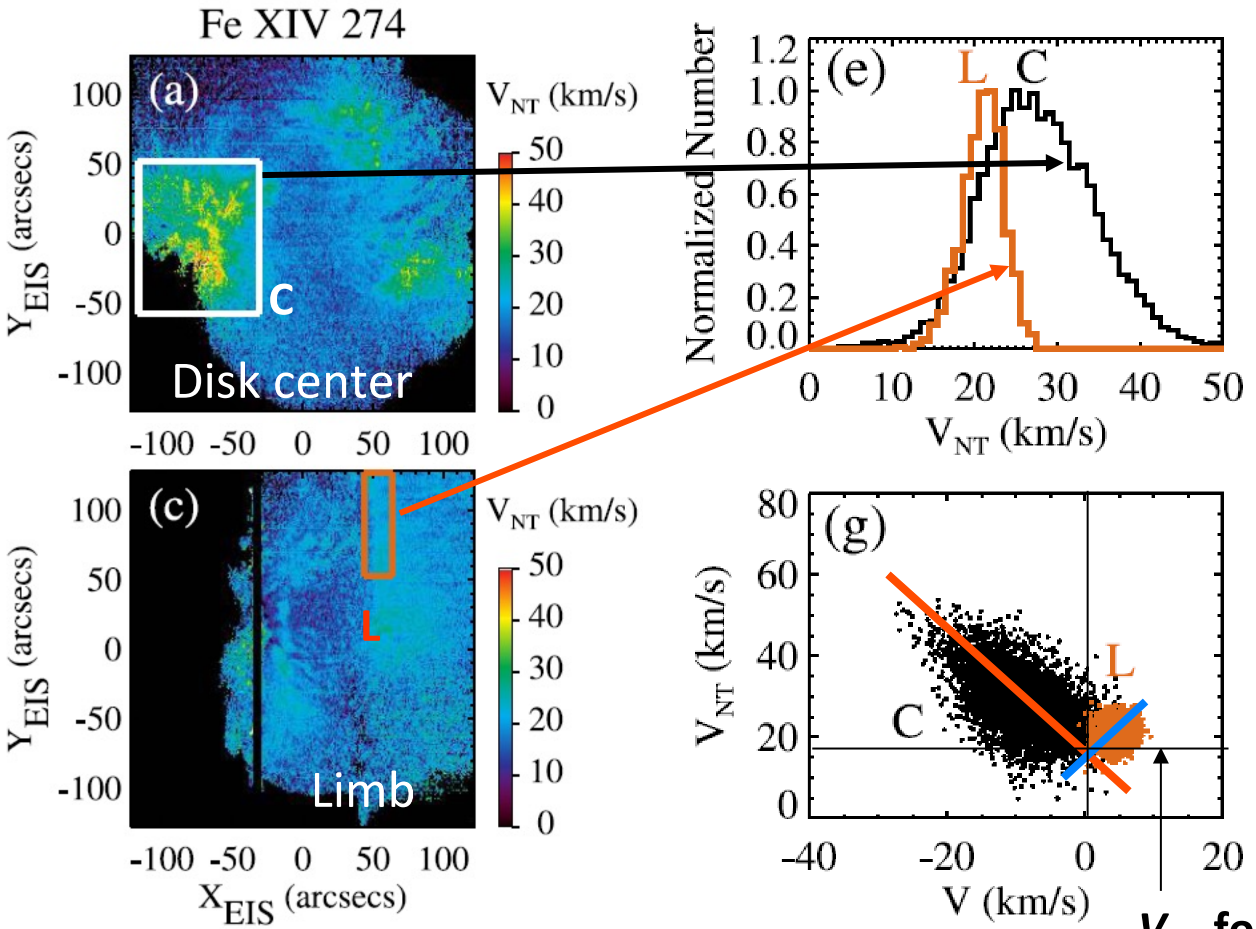

Histogram of V_{NT}

V_D – V_{NT} Scatter plot

V_{NT} for V_D=0

There is correlation between V and V_{NT}.

→ Superposition of line-of-sight plasma motions along magnetic field lines

Unresolved Doppler components are hidden !

Hara et al. 2008, ApJ, 678, L67

Blue-side Enhanced Line Profile

Line profiles at loop footpoints

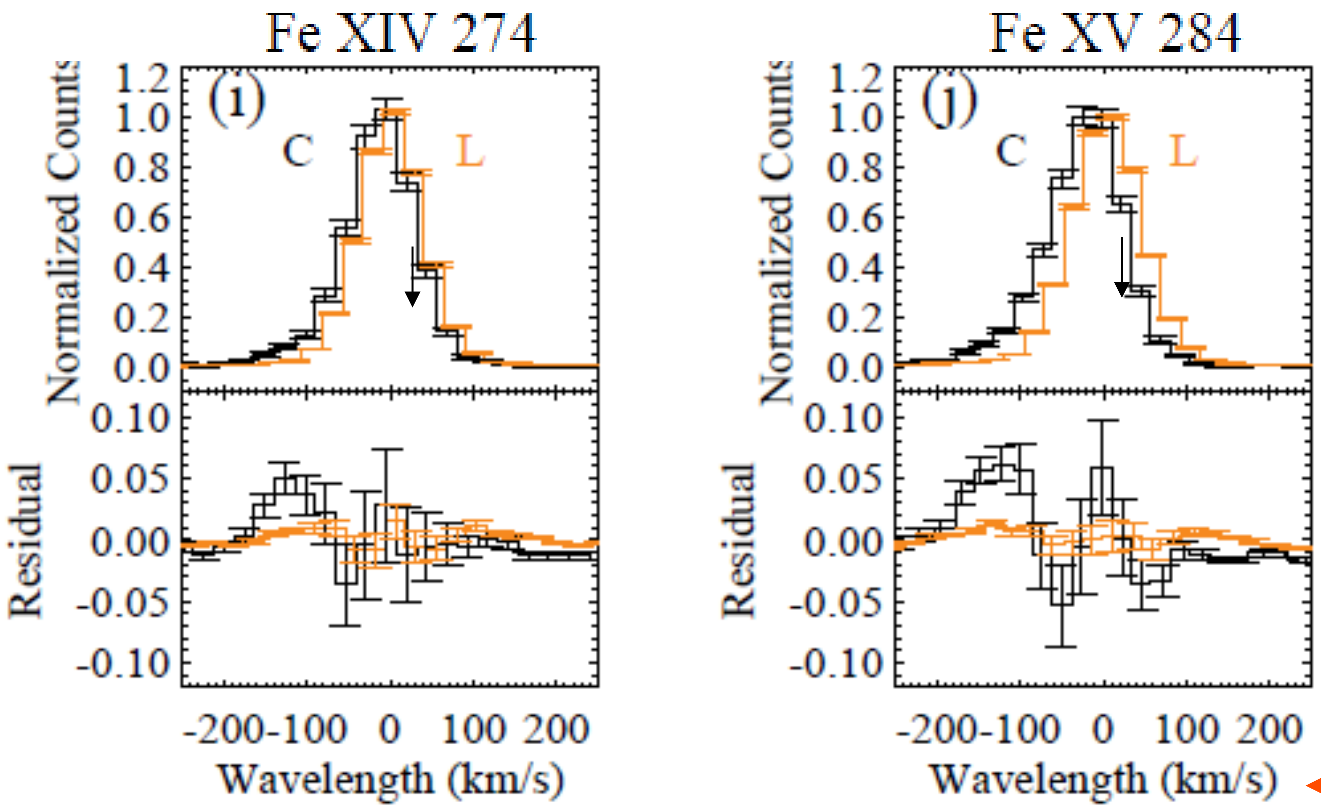

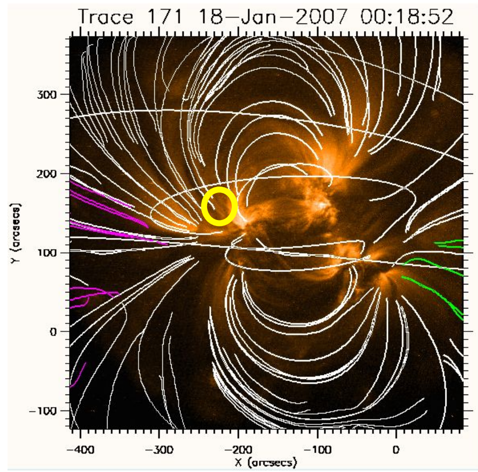

C: disk center

L: limb

$$V_D = \left(\frac{\lambda - \lambda_c}{\lambda_c} \right) c$$

Clearly showing the presence of unresolved high-velocity upflow components that have weaker emission than primary component.

$V_D / \cos\theta$ > 200 km/s ~ V_s

Hara et al. 2008, ApJ, 678, L67

Data & Analysis for V_{NT} Studies

- Hinode EIS data
- Long exposure (~ 1 min)
- Regions near the disk center and near the limb
- Single Gaussian approx. for line profile analysis
- Active/Quiescent (with/no microflares) active region

- Statistical studies not finished

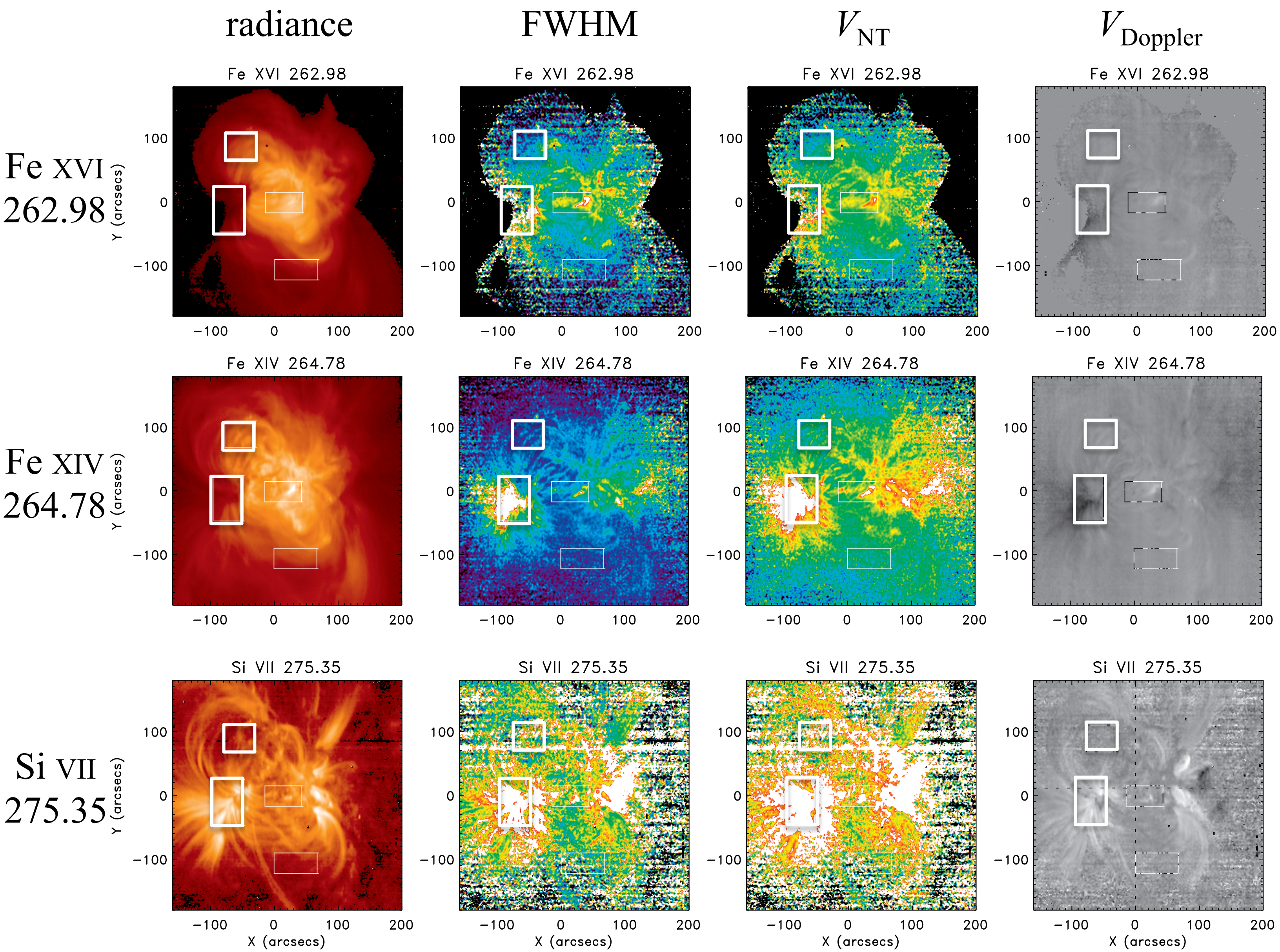

radiance
FWHM
V_{NT}
$V_{Doppler}$
Fe XVI 262.98
Fe XIV 264.78
Si VII 275.35
Fe XVI 262.98
Fe XIV 264.78
Si VII 275.35
Y (arcsecs)
X (arcsecs)

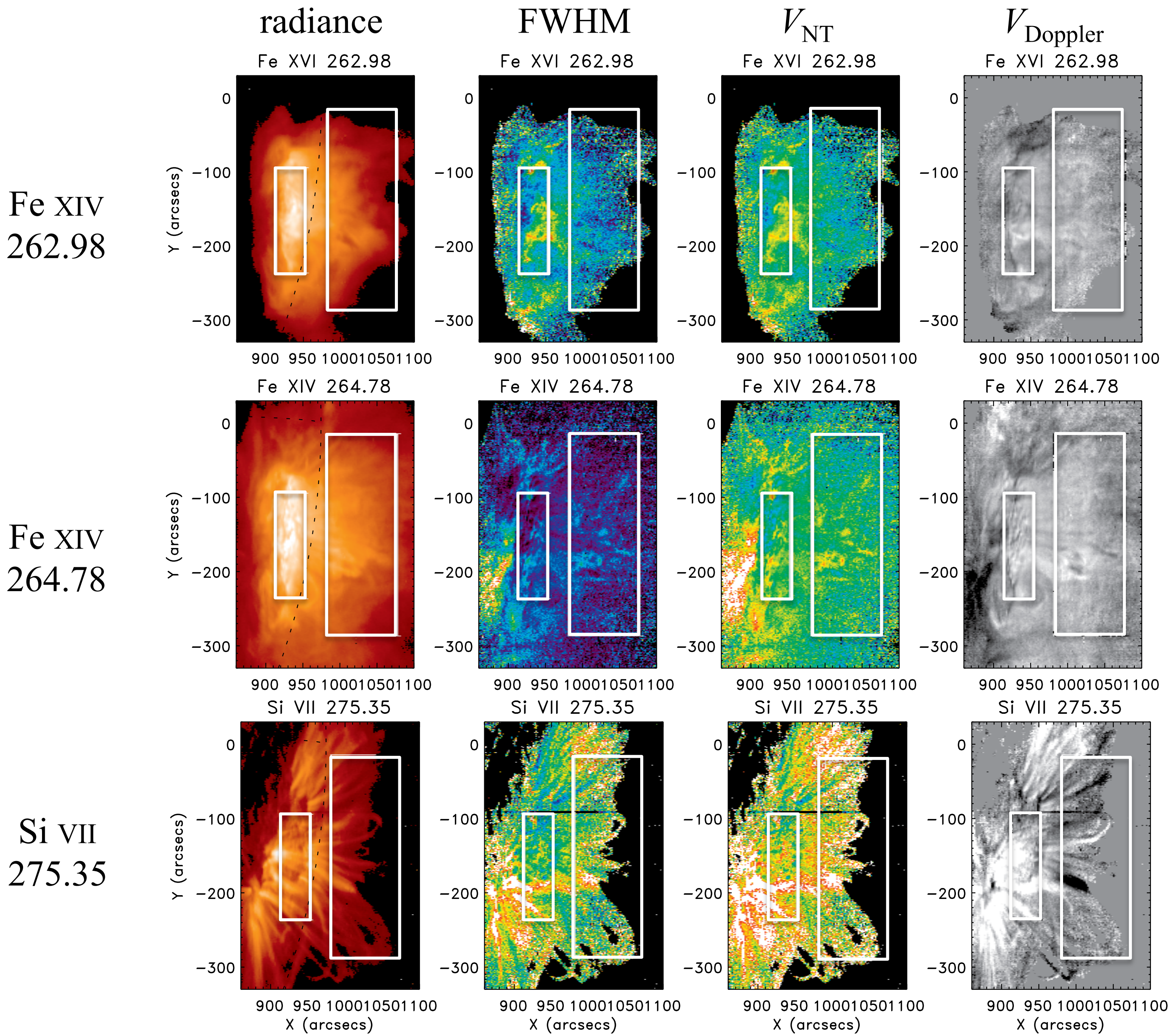

radiance
FWHM
V_{NT}
$V_{Doppler}$
Fe XIV 262.98
Fe XIV 264.78
Si VII 275.35
Fe XVI 262.98
Fe XIV 264.78
Si VII 275.35
Y (arcsecs)
X (arcsecs)
0
−100
−200
−300
900 950 1000 1050 1100

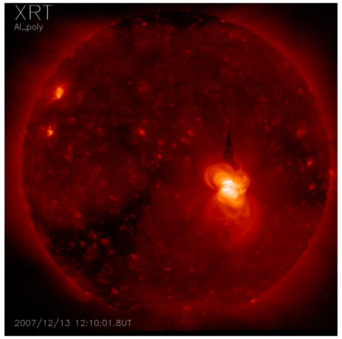

V_{NT}: Loops & Footpoints

20071213
(disk)

V_D - V_{NT}

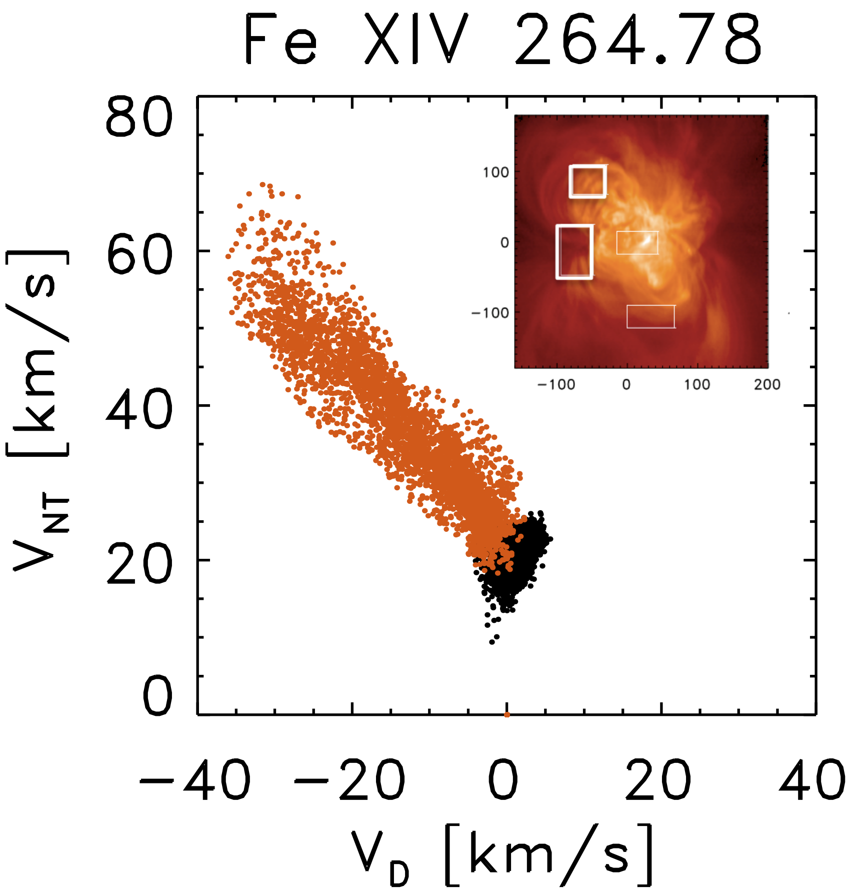

V_{NT} histogram

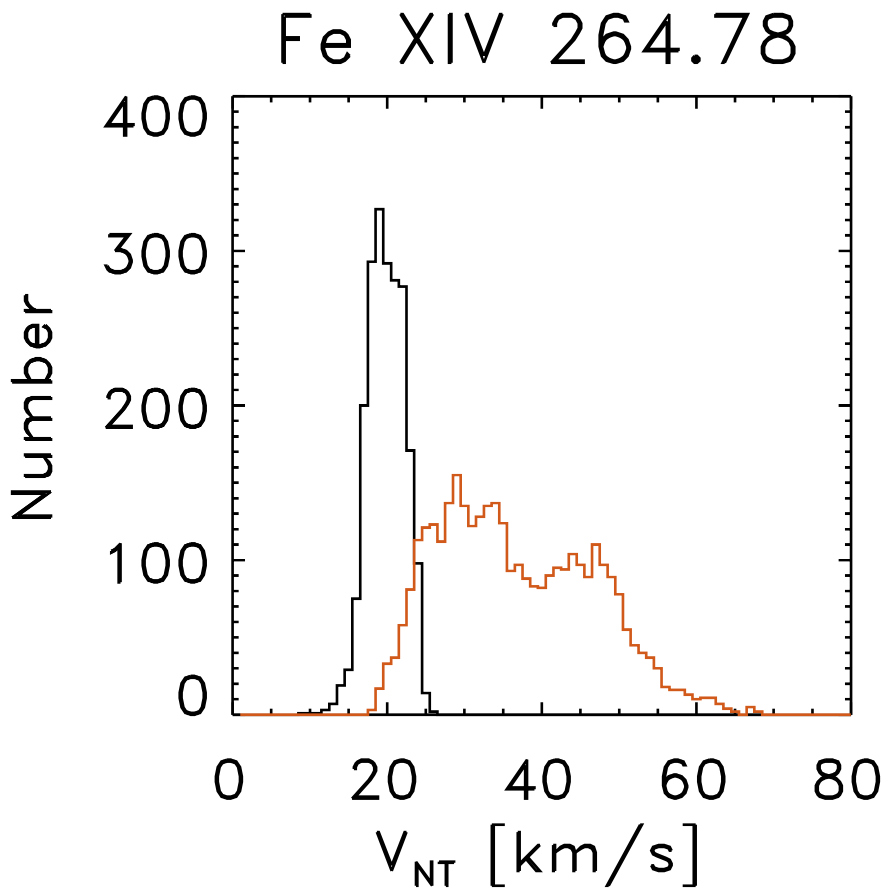

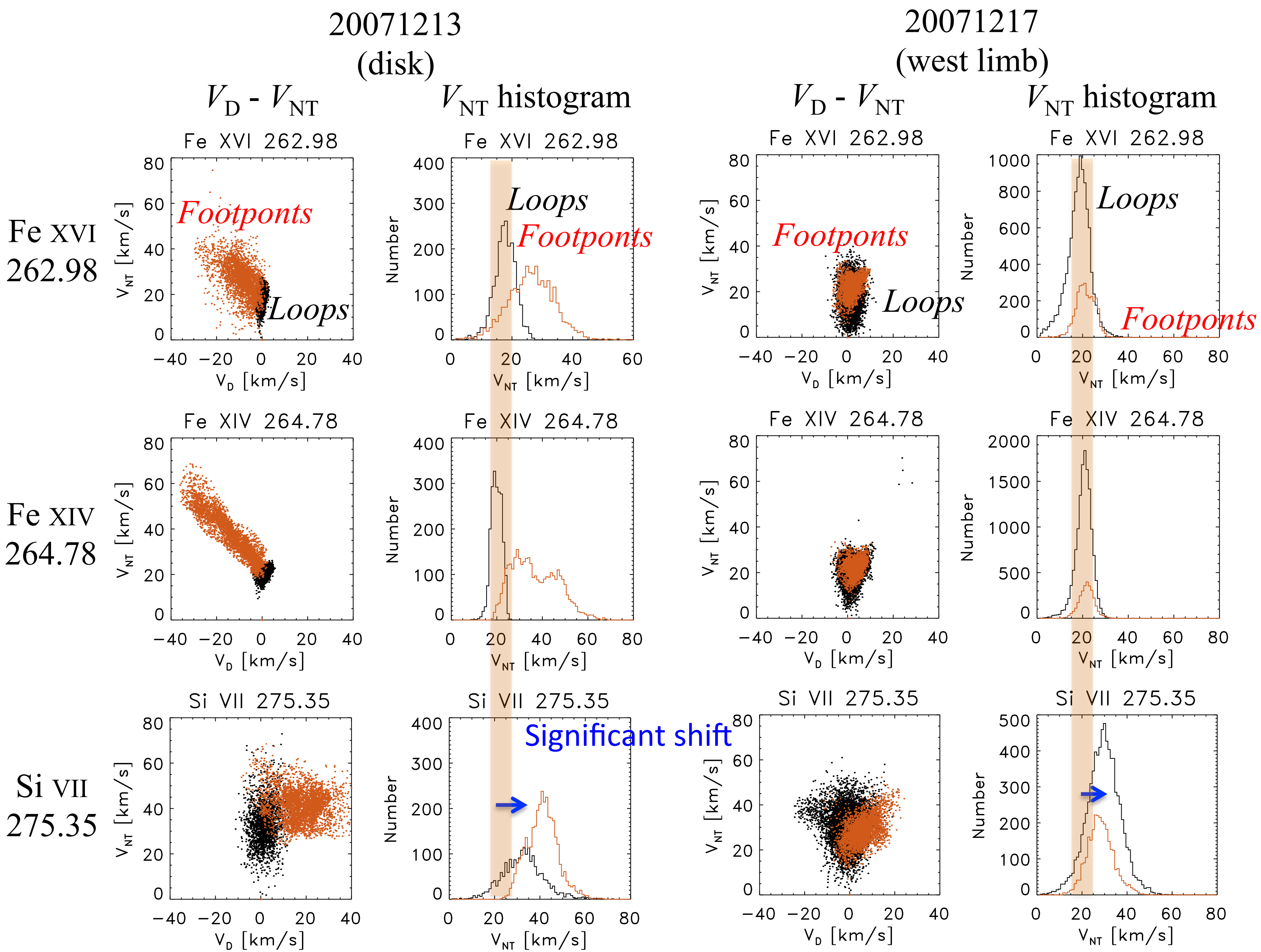

20071213
(disk)
20071217
(west limb)
VD - VNT
VNT histogram
Fe XVI 262.98
Fe XIV 264.78
Si VII 275.35
Footponts
Loops
Significant shift
VNT [km/s]
VD [km/s]
Number

Nonthermal velocity in emission lines

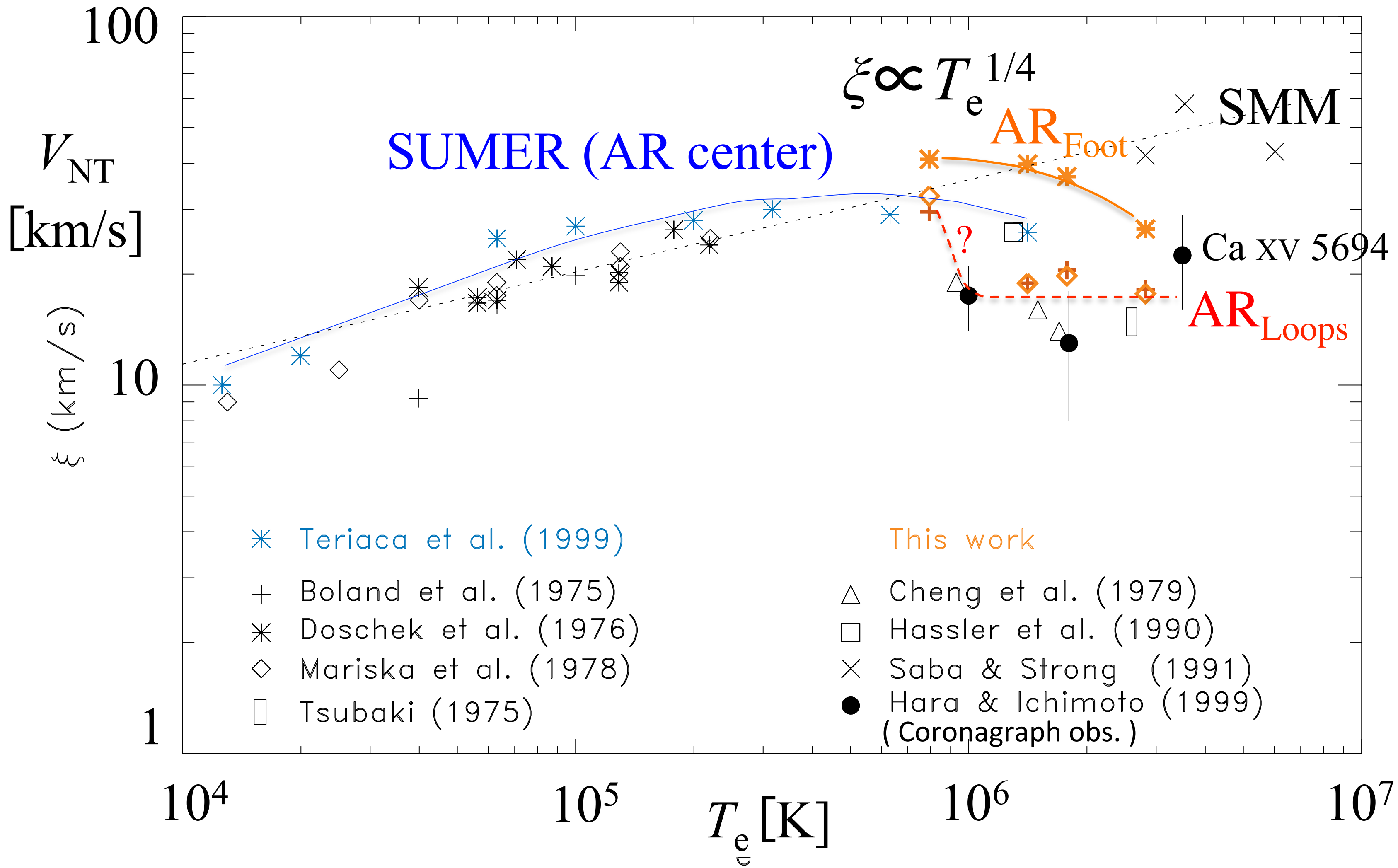

A search for Alfven waves/turbulence

Loop-top region

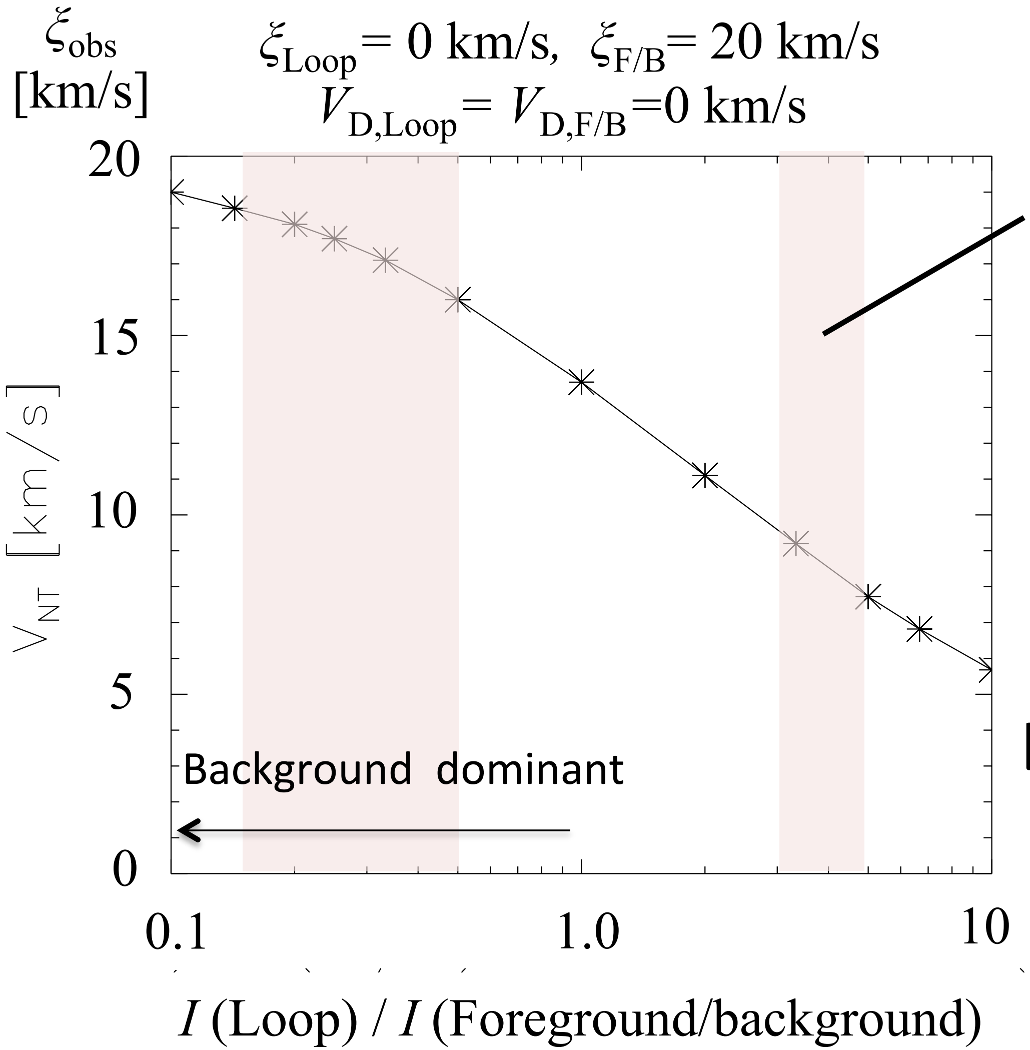

Study by Fe X/Fe XIV postflare loops by Hara & Ichimoto (1999) with a coronagraph of $\lambda/\Delta\lambda = 1\times10^5$

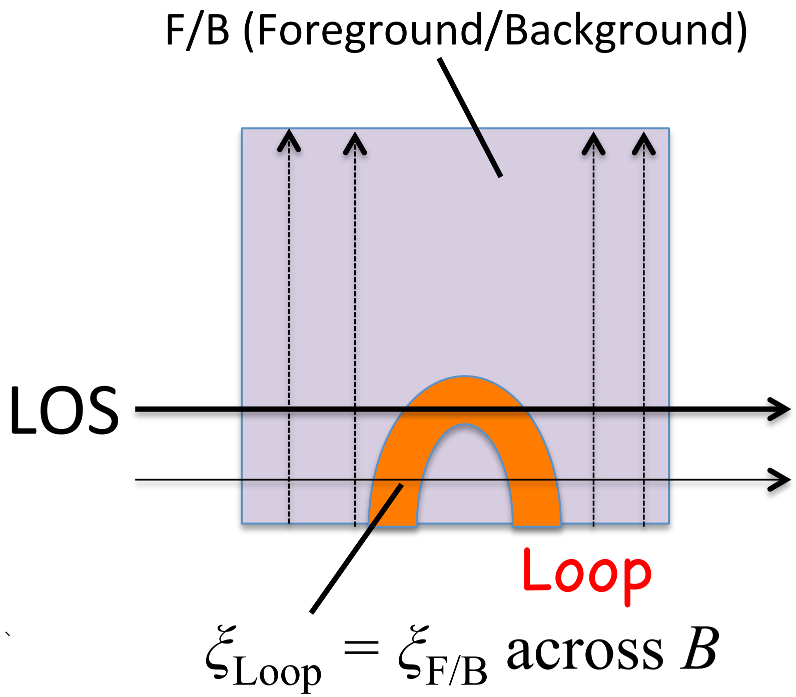

Previous Study

Fe XIV 5303
Coronal Green Line

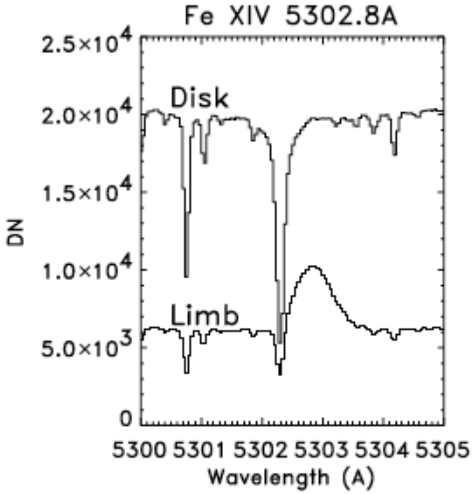

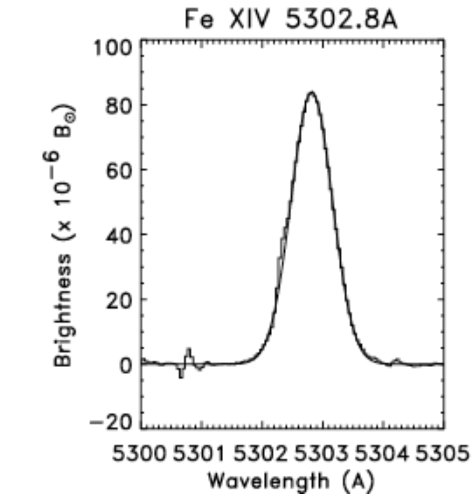

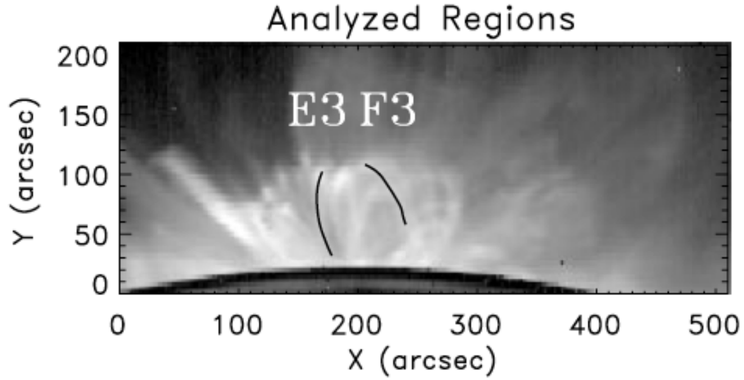

I along Loop

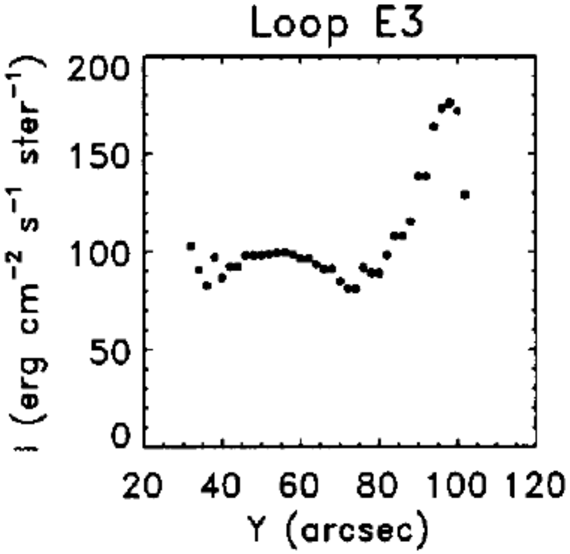

V_{NT} along Loop

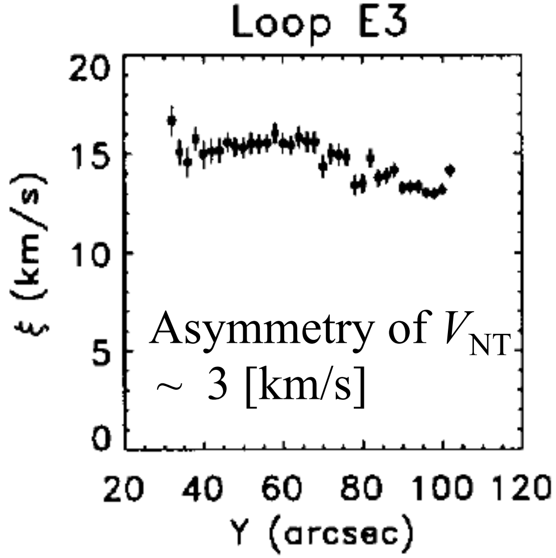

Asymmetry of V_{NT}
$\sim$ 3 [km/s]

Hara & Ichimoto (1999)

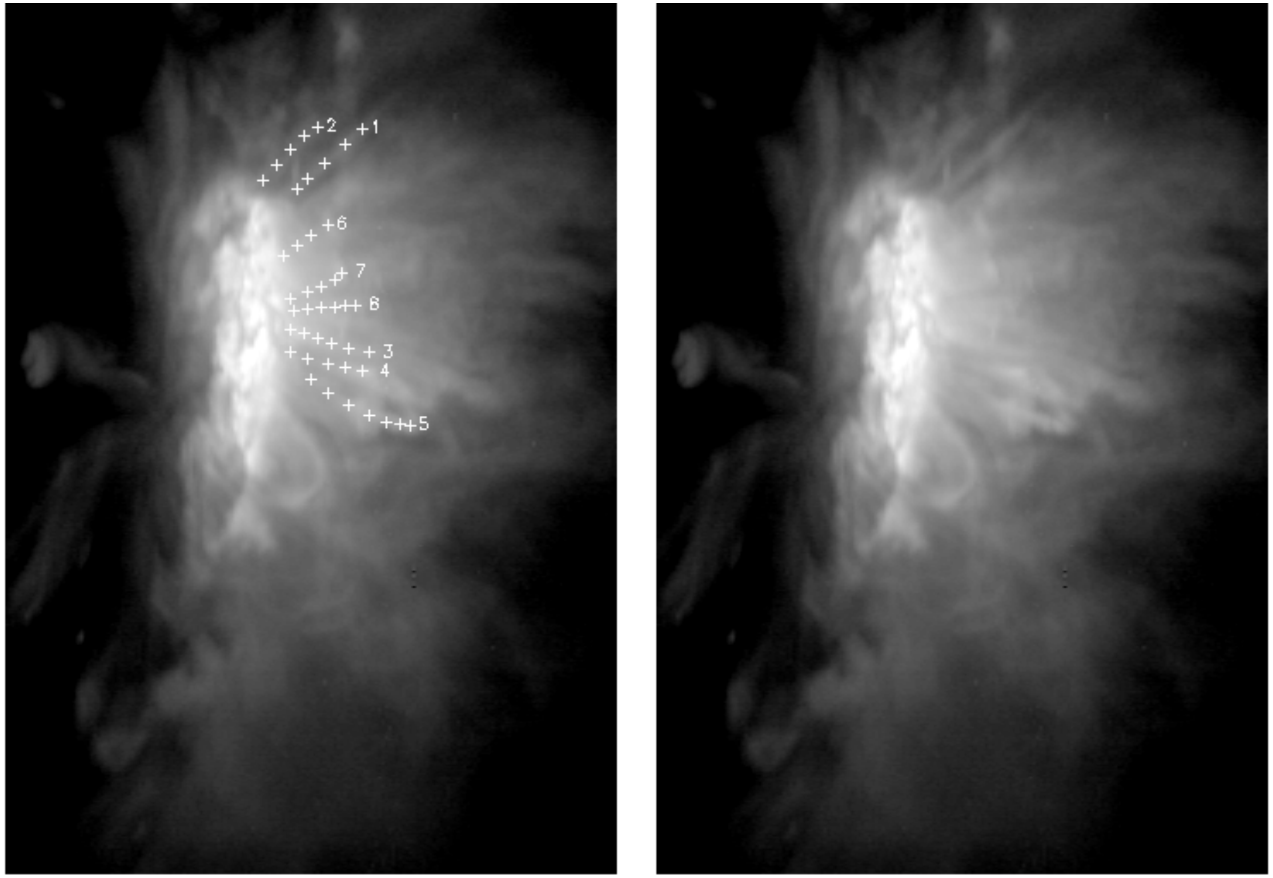
2
1
6
7
8
3
4
5

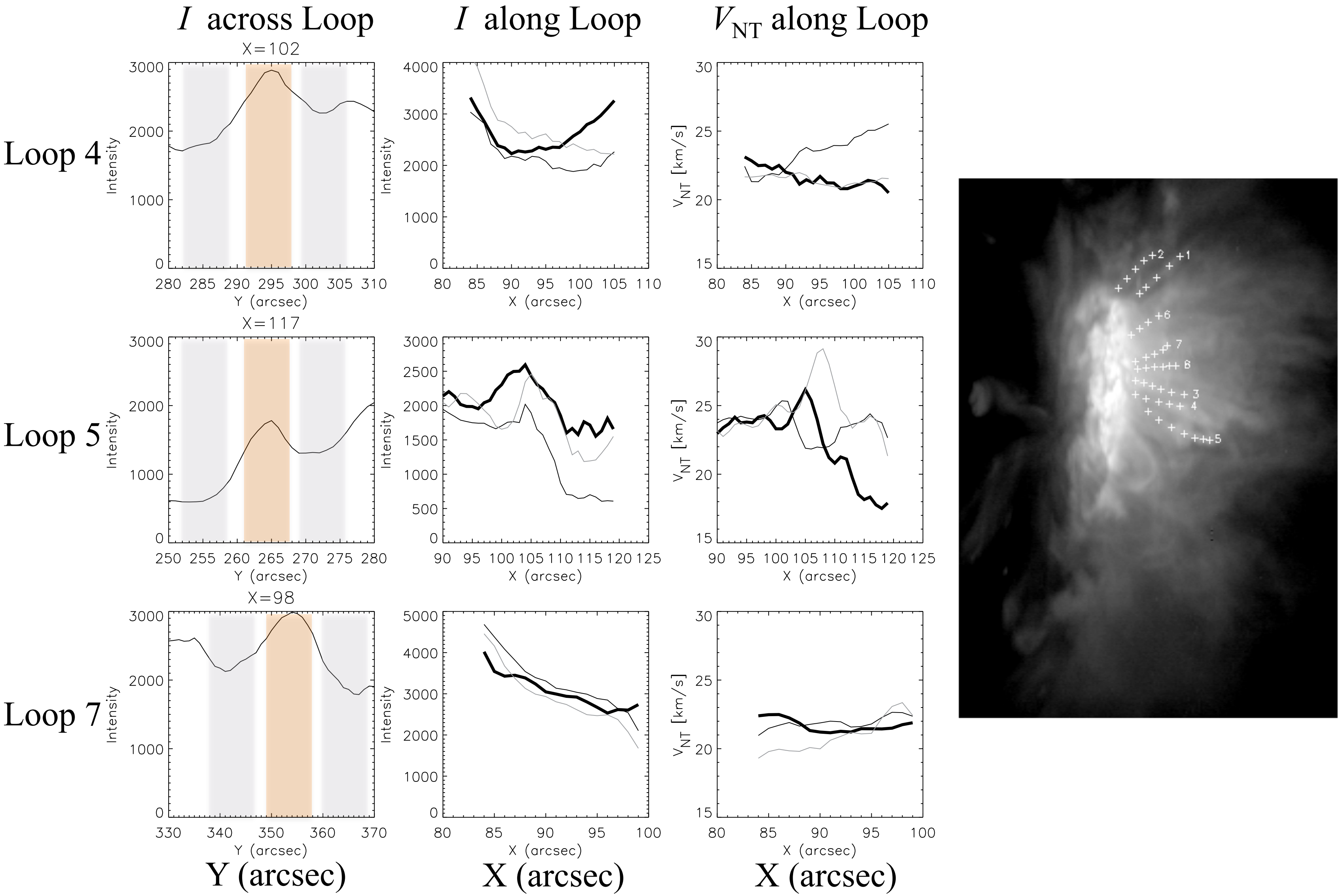

I across Loop
I along Loop
V_NT along Loop
Loop 4
Loop 5
Loop 7
X=102
X=117
X=98
Intensity
V_NT [km/s]
Y (arcsec)
X (arcsec)
1
2
3
4
5
6
7
8

Conclusions

- We have analyzed the Hinode EIS spectral data to investigate the line-width change and anisotropy in active-region structures of log T_e= 5.9 - 6.4.
  - Strong anisotropy at footpoints as have been found in 2008
  - A very weak anisotropy/nearly none in the loop structures
  - Need interpretations for large V_{NT} in Si VII loops.
    - Not at the interface region between chromosphere & corona. IRIS observations will be a help for understanding.

- Line-width change with height along coronal loops found from visible green line (Fe XIV) (Hara & Ichimoto 1999, Singh+2003) has also been found from EIS data.
  - Line-width along coronal loops decreases with height in Fe XIV, but it appears to be strongly affected by foreground/background and dynamic structures because I_{loop} / $I_{F/B}$ is small: (A view of steadiness misleads interpretations.)
  - Evidence for Alfven waves/Alfven-wave turbulence is not easy to detect in the data set we used this time. Need more case studies.